


Article

# A Very Low Complexity QRD-M MIMO Detection Based on Adaptive Search Area

Bong-seok Kim <sup>1</sup>, Sang-Dong Kim <sup>1</sup>, Dongjun Na <sup>2</sup> and Kwonhue Choi <sup>2,\*</sup>

<sup>1</sup> Daegu Gyeongbuk Institute of Science and Technology (DGIST), Daegu 42988, Korea; remnant@dgist.ac.kr (B.-s.K.); kimsd728@dgist.ac.kr (S.-D.K.)

<sup>2</sup> Department of Mobile Information & Communication Engineering, Yeungnam University, Gyeongsan 38541, Korea; nadj2964@ynu.ac.kr

\* Correspondence: gonew@yu.ac.kr; Tel.: +82-53-810-3516

Received: 17 April 2020; Accepted: 2 May 2020; Published: 4 May 2020



**Abstract:** We propose a low complexity QR decomposition (QRD)-M multiple input multiple output (MIMO) detection algorithm based on adaptive search area. Unlike the conventional QRD-M MIMO detection algorithm, which determines the next survivor path candidates after searching over the entire constellation points at each detection layer, the proposed algorithm adaptively restricts the search area to the minimal neighboring constellation points of the estimated QRD symbol according to the instantaneous channel condition at each layer. First, we set up an adaptation rule for search area using two observations that inherently reflect the instantaneous channel condition, that is, the diagonal terms of the channel upper triangle matrix after QR decomposition and Euclidean distance between the received symbol vector and temporarily estimated symbol vector by QRD detection. In addition, it is found that the performance of the QRD-M algorithm degrades when the diagonal terms of the channel upper triangle matrix instantaneously decrease. To overcome this problem, the proposed algorithm employs the ratio of each diagonal term and total diagonal terms. Moreover, the proposed algorithm further decreases redundant complexity by considering the location of initial detection symbol in constellation. By doing so, the proposed algorithm effectively achieves performance near to the maximum likelihood detection algorithm, while maintaining the overall average computation complexity much lower than that of the conventional QRD-M systems. Especially, the proposed algorithm achieves reduction of 76% and 26% computational complexity with low signal to noise ratio (SNR) and high SNR, compared with the adaptive QRD-M algorithm based on noise power. Moreover, simulation results show that the proposed algorithm achieves both low complexity and lower symbol error rate compared with the fixed QRD-M algorithms.

**Keywords:** long term evolution advanced (LTE-A); multiple input multiple output (MIMO); QRD-M; low complexity algorithm

## 1. Introduction

Multiple input multiple output (MIMO) systems have received significant attention, owing to the rapid development of high-speed broadband wireless communication systems employing multiple transmit and receive antennas [1–12]. MIMO systems have many advantages such as spatial diversity and high throughput without increasing bandwidth. Thus, MIMO systems are employed in modern and next generation wireless standards [1].

Meanwhile, there are many challenging issues to overcome from disadvantages owing to increasing of the number of antennas. For example, multi-user MIMO systems have been studied in [2–8]. In [2] and [3], the authors tried to maximize signal to interference plus noise ratio by employing the precoding schemes to minimize interference among multiple users. In [4], an adaptive antennas algorithm at the

mobile and base stations has been proposed. In [6], they proposed a near optimal scheduling algorithm by managing radio resource for multi-user MIMO systems.

Meanwhile, studies to solve the problems of mutual coupling between multiple antennas are receiving much attention [9–12]. In [9], the authors designed a compact dual band-notched ultra wideband MIMO antenna in order to achieve high isolation. In [10], the authors presented a slot structure perpendicular to current on the surface of patches to overcome the mutual coupling problems. In [11], the authors tried to reduce the mutual coupling between closely packed antenna elements using defected ground structure.

As one of the most promising among the challenging issues for MIMO systems, the complexity reduction of MIMO detection algorithms has recently been studied [13–22]. The optimal detector for MIMO system is the maximum likelihood detection (MLD) algorithm. However, MLD requires exponential complexity regarding the number of transmit antennas [1]. Recently, several algorithms achieving near-MLD performance have been proposed for MIMO systems [16–21]. The tree search based QR decomposition (QRD)- $M$  algorithm and sphere decoding (SD) achieve near-MLD performance, while requiring substantially low complexity in comparison with MLD.

The fixed QRD- $M$  algorithm compromises the complexity and performance by selecting only  $M$  survivor paths among all possible paths at each layer of the tree search [16,17]. The metric computational complexity is determined by the product of  $M$  and the number of the candidate symbols in the next detection layer,  $S$ , which has been conventionally set to be the number of all constellation points  $C$ . To achieve near-MLD performance for this algorithm, the value of  $M$  and  $S$  should be large enough for the selected paths to include the correct path. This still requires high computational complexity. Recently, in [18], a low complexity QRD- $M$  algorithm was proposed by reducing the redundant metric computation complexity with identical performance at the first and the last detection layer. However, this algorithm still has inefficient computation complexity because  $M$  and  $S$  are fixed regardless of the instantaneous channel condition. If  $M$  or  $S$  is adaptively controlled according to the instantaneous channel condition, the computational complexity should be effectively decreased compared with the conventional fixed QRD- $M$  algorithm.

Recently, adaptive QRD- $M$  algorithms based on average noise power have been proposed [19–21]. They can be classified as two kinds of adaptation algorithms. One is the adaptation of  $M$  and the other one is the adaptation of  $S$ . The conventional adaptive QRD- $M$  algorithms control the number of survivor paths,  $M$ , according to average noise power [19,20]. On the other hand, the conventional adaptive search area QRD- $M$  algorithm adaptively changes  $S$  according to SNR [21]. We will call the QRD- $M$  algorithm with the adaptation of  $S$  the adaptive search area QRD- $M$  algorithm in other words. The simulation results reveal that adaptive search area QRD- $M$  algorithm enables us to more drastically reduce the computational complexity than the conventional adaptive QRD- $M$  algorithm. This implies that reducing the search area (candidate path space size) is safer than reducing the number of survivor paths in order to reduce the computation complexity without losing the correct path. However, the adaptive search area QRD- $M$  algorithm in [21] still has a problem. This algorithm cannot adaptively change the search area,  $S$ , against the instantaneous variation of the channel condition, because this algorithm controls  $S$  based on the average noise power.

In this paper, we propose an adaptive search area QRD- $M$  algorithm that overcomes the complexity reduction limit of the conventional adaptive search area QRD- $M$  algorithm. The proposed algorithm accomplishes dynamic adaptation of  $S$  by observing the diagonal terms of the channel upper triangle matrix after QR decomposition and Euclidean distance between the received signal vector and temporarily estimated symbol vector by QRD. These two observations are found to form a good indicator of the instantaneous channel condition because they are the simple functions of the instantaneous noise sample power as well as the instantaneous channel fading magnitudes and correlation. First, we propose a simple, but efficient instantaneous channel condition indicator formula using these two observations, and then we show that, based on the proposed channel indicator, a very tight adaptive setting of search area is possible without performance loss. In addition, it is found that the performance of the QRD- $M$

algorithm degrades when the diagonal terms of the channel upper triangle matrix instantaneously decrease. To overcome this problem, the proposed algorithm employs ratio of each diagonal term and total diagonal terms. Moreover, the proposed algorithm further decreases redundant complexity by considering the location of initial detection symbol in constellation. By doing so, the proposed algorithm effectively achieves performance near to the maximum likelihood detection algorithm, while maintaining the overall average computation complexity much lower than that of the conventional QRD-M systems. Especially, the proposed algorithm achieves reduction of 76% and 26% computational complexity with low signal to noise ratio (SNR) and high SNR, respectively, compared with the adaptive QRD-M algorithm based on noise power. Moreover, the simulation results show that the proposed algorithm achieves both low complexity and lower symbol error rate compared with the fixed QRD-M algorithms. As a result, the proposed algorithm efficiently decreases the computation complexity without performance degradation compared with the conventional adaptive search area QRD-M algorithm.

The remainder of the paper is organized as follows. Section 2 describes the system model considered in this paper, and Sections 3 and 4 explain the conventional QRD-M algorithm and the adaptive search area QRD-M algorithm. The proposed low complexity QRD-M algorithm is introduced in Section 5. In Section 6, the performance and complexity of the proposed algorithm are evaluated through computer simulations. Finally, we present the conclusion in Section 7.

## 2. System Model

We consider a MIMO system that consists of  $N$  transmit (TX) and  $L$  receive (RX) antennas, as shown Figure 1. The received signal vector  $\mathbf{y}$  is described by

$$\mathbf{y} = \mathbf{H}\mathbf{s} + \mathbf{w} \tag{1}$$

where  $\mathbf{s}$  is  $N$ -dimensional TX symbol vector,  $\mathbf{H}$  is the  $L \times N$  channel matrix, and  $\mathbf{w}$  is  $L$  dimensional complex additive white Gaussian noise (AWGN) vector with zero mean and variance, and (1) is rewritten as follows:

$$\begin{bmatrix} y_1 \\ y_2 \\ \vdots \\ y_L \end{bmatrix} = \begin{bmatrix} h_{1,1} & h_{1,2} & h_{1,3} & \dots & h_{1,N} \\ h_{2,1} & h_{2,2} & h_{2,3} & \dots & h_{2,N} \\ \vdots & \vdots & \vdots & \ddots & \vdots \\ h_{L,1} & h_{L,2} & h_{L,3} & \dots & h_{L,N} \end{bmatrix} \begin{bmatrix} s_1 \\ s_2 \\ \vdots \\ s_N \end{bmatrix} + \begin{bmatrix} w_1 \\ w_2 \\ \vdots \\ w_L \end{bmatrix} \tag{2}$$

where  $y_l$  is the  $l$  th RX symbol, that is,  $\mathbf{y} = [y_1, y_2, \dots, y_L]^T$ , where  $(\cdot)^T$  is transpose operator and  $h_{l,n}$  is the element  $l$  th and  $n$  th of  $\mathbf{H}$ ; and  $s_n$  is the  $n$  th TX symbol, that is,  $\mathbf{s} = [s_1, s_2, \dots, s_N]^T$ . Each element of symbol vector  $\mathbf{s}$  is chosen from the quadrature amplitude modulation (QAM) constellation with the average symbol energy, which is denoted by  $E_s$ . We consider a Rayleigh fading where the elements of  $\mathbf{H}$  are independent complex Gaussian with zero mean and unit variance. It is assumed that the channel matrix  $\mathbf{H}$  is known by the receiver and remains constant over the data symbol duration.

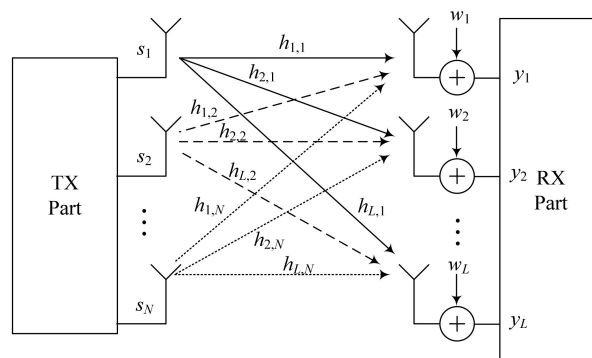


**Figure 1.** Structure of multiple input multiple output (MIMO) systems with  $N$  transmit (TX) and  $L$  receive (RX) antennas.

### 3. Conventional Fixed QRD-M Algorithm

The conventional fixed QRD-M algorithm is based on the classical  $M$ -algorithm [16,17]. At each detection layer, instead of deciding the transmitted symbol, QRD-M algorithm keeps  $M$  reliable survivor paths. First, performing QR-decomposition on  $H$ , we obtain

$$H = QR \tag{3}$$

where  $Q$  is a  $L \times L$  unitary matrix and  $R$  is  $N \times N$  upper triangular matrix. Noting that,  $Q^H Q = I$ , where  $I$  is the identity matrix and  $Q^H$  is the conjugate transpose of  $Q$ . After pre-Multiplying received signal by  $Q^H$ , we can rewrite (1) as follows:

$$\tilde{y} = RS + \tilde{n} \tag{4}$$

where  $\tilde{y}$  is  $Q^H y$  and  $\tilde{n}$  is  $Q^H n$ . It follows from (4) that

$$\begin{aligned} \tilde{y}_1 &= r_{1,1}s_1 + r_{1,2}s_2 + r_{1,3}s_3 + \dots + r_{1,N}s_N + \tilde{n}_1 \\ \tilde{y}_2 &= r_{2,2}s_2 + r_{2,3}s_3 + \dots + r_{2,N}s_N + \tilde{n}_2 \\ &\vdots \\ \tilde{y}_{N-1} &= r_{N-1,N-1}s_{N-1} + r_{N-1,N}s_N + \tilde{n}_{N-1} \\ \tilde{y}_N &= r_{N,N}s_N + \tilde{n}_N \end{aligned} \tag{5}$$

where  $\tilde{y}_i$  is the  $i$ -th element of vector  $\tilde{y}$ , and  $r_{j,i}$  is the element of the  $j$ -th row and the  $i$ -th column of  $R$  and  $r_{j,i} = 0$  when  $j > i$ .

From (5), the signal detection can be realized through a tree searching process from  $s_N$  to  $s_1$ , where  $s_N$  and  $s_1$  are the last and the first element of  $s$ , respectively. In the conventional QRD-M algorithm, only  $M$ -paths will survive in each detection layer according to the accumulated Euclidean distances on different paths. In the first detection layer ( $N$ -th row in  $R$ ), path metrics  $u_N$  are calculated as follows:

$$u_N = \|\tilde{y}_N - r_{N,N}\tilde{s}_N(m)\|^2 \tag{6}$$

where  $\tilde{s}_N(m)$  is the  $m$ -th candidate of  $s_N$ . The accumulated Euclidean distance of the  $m$ -th path in the  $i$ -th detection layer (=  $(N - i + 1)$ th row in  $R$ ) is calculated as follows:

$$u_{N-i+1} = \sum_{j=1}^i \left\| \tilde{y}_{N-j+1} - \sum_{k=N-j+1}^N r_{N-j+1,k}\tilde{s}_k(m) \right\|^2, \tag{7}$$

where  $\tilde{s}_k(m)$  is the candidate of  $s_k$  on the  $m$ -th path. Figure 2 shows an example of the conventional QRD-M algorithm ( $M = 4$ ) with  $N = L = 4$ , and quadrature phase shift keying (QPSK). The number of layers is equal to  $N$ , and  $M$  nodes are maintained at each layer. The minimum path metric is chosen as an estimation symbol vector,  $\hat{s}$  at the last layer.

At the final detection layer ( $i = N$ ), the candidate vector that corresponds to the minimum path metric value is chosen as the detection signal set.

As the detection process spends its computation time mainly on metric computations, we take the number of metric computations as the complexity measure. If we denote  $T_{\text{fixed}}$  as the number of metric computations of the conventional QRD-M algorithm, it is calculated as follows:

$$T_{\text{fixed}} = C + MC(N - 1). \tag{8}$$

Recently, a reduced complexity QRD- $M$  algorithm has been proposed in [18]. They avoid the redundant computation at the first and the final layers with identical performance. The number of metric computations of this reduced algorithm,  $T_{\text{reduced}}$  is calculated as follows:

$$T_{\text{reduced}} = MC(N - 2). \tag{9}$$

From (8) and (9), we note that the metric computational complexity of the conventional QRD- $M$  algorithm is roughly determined by the product of  $M$ ,  $C$ , and  $N$ , and this is much smaller than that of MLD, which is given as  $C^N$ . However, if we want to make the performance of the conventional QRD- $M$  algorithm approach that of MLD, we need a considerably large value of  $M$  for the worst case design.

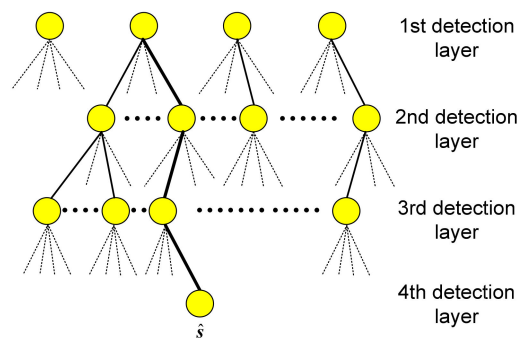


**Figure 2.** An example of the conventional QRD (QR decomposition)- $M$  ( $M = 4$ ) with  $N = L = 4$  and quadrature phase shift keying quadrature phase shift keying (QPSK).

#### 4. SNR-Based Adaptive Search Area QRD- $M$ Algorithm

The adaptive search area QRD- $M$  algorithm has been proposed in order to further reduce the complexity of the conventional fixed QRD- $M$  algorithms [21]. In this algorithm, the number of extended nodes per survivor path  $S$  is adaptively changed according to average noise power instead of all constellation points  $C$ , at step 4 in the previous section. That is, the  $S$  closest constellation points from the soft decision symbol by QRD are chosen at each layer. The soft decision by QRD at the  $i$ -th detection layer is denoted by  $d^{[i]}$  and is calculated as follows:

$$d^{[i]} = \left( \tilde{y}_{N-i+1} - \sum_{k=N-i+2}^N r_{N-i+1,k} \cdot \tilde{s}_k \right) / r_{N-i+1,N-i+1}. \tag{10}$$

Figure 3 shows an example of the closest order of the constellation points with 16 QAM plane from  $d^{[i]}$ . The numbers in parentheses mean the closest order from  $d^{[i]}$ .

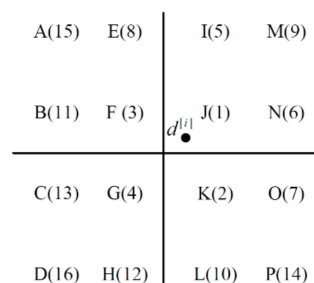


**Figure 3.** Example of the closest order of the constellation points with 16 quadrature amplitude modulation (QAM) from  $d^{[i]}$ .

The probability that the correct path’s metric is not included among the smallest  $S$  path metrics can be approximated by the probability of event  $A$  that the correct hypothesis falls outside of the

square box that centers at  $d^{[i]}$ , and encloses  $S$  constellation points. Assuming the constellation is sufficiently large such that the continuous approximation [21] holds and the effects of points at the edge of the constellation are negligible, the side of such a box is  $2\sqrt{S^{[i]}/4D'_{\min}}$ , where  $S^{[i]}$  is  $S$  at the  $i$ -th detection layer and  $D_{\min}$  and  $D'_{\min,i} \triangleq \gamma_i D_{\min}$  are the minimum distances of the transmitted and received constellations, respectively ( $\gamma_i \triangleq r_{N-i+1,N-i+1}$ ). Setting  $\Pr(A) \leq P_t$  to achieve the specified performance level, where  $P_t$  is pre-specified target level and using the assumption that each entry of  $w$  is an i.i.d. Gaussian r.v. with zero mean and variance,  $\sigma^2$ , we have

$$\Pr(A) = 1 - \left[ 1 - 2Q\left(\sqrt{S^{[i]}/4D'_{\min}}\right) \right]^2 \leq P_t \tag{11}$$

where  $Q(x) \triangleq 1/\sqrt{2\pi} \int_x^\infty e^{-\tau^2/2} d\tau$ . With moderate to high SNRs, the second-order term of the  $Q$ -function in (11) can be ignored. Furthermore, let  $S_{\max}$  denote the largest allowable value of  $S^{[i]}$  that is set by the implementation constraints and the size of constellation, that is,  $S_{\max} \leq |C|$ . It follows that the minimum integer value for  $S^{[i]}$  that satisfies (11) and the constraints in complexity and constellation size is found to be as follows:

$$S_{\text{raw}}^{[i]} = \min \left\{ \left\lceil 4 \left[ \frac{\sigma}{\sqrt{2}d'_{\min}} Q^{-1}\left(\frac{P_t}{4}\right) \right]^2 \right\rceil, S_{\max} \right\} \tag{12}$$

where  $\lceil x \rceil$  is the smallest integer that is greater than or equal to  $x$ . Finally, to enable set partitioning,  $S^{[i]}$  is set to

$$S^{[i]} = \left\lceil S_{\text{raw}}^{[i]} \right\rceil_2 \tag{13}$$

where  $\lceil \cdot \rceil_2$  is the operation that rounds up to the nearest integer that is a power of 2. The number of considered candidate symbols,  $S^{[i]}$  can be set to 1, 2, 4, 8, and 16 with 16 QAM.

By adaptively controlling the size of the search area based on SNR, the computational complexity of this algorithm can be significant decreased compared with the conventional fixed QRD-M algorithm, which is set to  $S = C$  as the search area. However, this algorithm cannot adaptively change  $S^{[i]}$  against the instantaneous variation of the channel condition as this algorithm controls  $S^{[i]}$  based on the average SNR does not reflect the instantaneous channel information, such as the instantaneous channel fading and instantaneous noise sample power. Therefore, we have to accept either the increasing complexity or performance degradation, which is the main shortcoming of this algorithm.

### 5. Proposed Adaptive Search Area QRD-M Algorithm

In this section, we illustrate the proposed adaptive search area QRD-M algorithm, which controls  $S$  using the instantaneous channel condition instead of average noise power of the conventional adaptive search area QRD-M algorithm. The proposed algorithm is an advanced version of [22]. Compared with [22], the proposed algorithm employs additional channel indicator, that is, accumulated Euclidean distance at each layer in order to improve the performance and the average diagonal terms to reflect channel conditions of all the layers. The proposed algorithm uses diagonal elements of  $\mathbf{R}$  and Euclidean distance between the received symbol vector and the temporal QRD estimation symbol vector as a simple channel reliability indicator.

As one of channel indicators of the proposed scheme, we employ the ratio of power of diagonal term of channel matrix  $\mathbf{R}$  at the  $i$ -th detection layer, as shown in [17]. This indicator is denoted by  $\xi^{[i]}$  and is calculated as follows:

$$\xi^{[i]} = |r_{N-i+1,N-i+1}|^2 / \frac{1}{N} \sum_{k=1}^N |r_{k,k}|^2. \tag{14}$$

In the denominator in (14), the diagonal term is normalized by the average diagonal terms. This is because we intend to make this indicator  $\xi^{[i]}$  dependent on the variable channel matrix not on the



SNR in order to get rid of the signal scaling effect and measure the relative channel state with respect to all of the detection layers.

As another instantaneous channel indicator, we additively employ Euclidean distance between the temporarily estimated symbol by QRD  $\hat{s}_{N-i+1}^{QR}$  and the received signal  $\tilde{y}_{N-j+1}$  at  $i$ -th detection layer. The accumulated Euclidean distance between  $\tilde{y}_{N-j+1}$  and  $\hat{s}_{N-i+1}^{QR}$  is denoted by  $u^{QR}$  and is calculated as follows:

$$u^{QR} = \sum_{j=1}^N \left\| \tilde{y}_{N-j+1} - \sum_{k=N-j+1}^N r_{N-j+1,k} \hat{s}_k^{QR} \right\|^2 \tag{15}$$

If  $\hat{s}_k^{QR}$  is the correct detection symbol, there remains only noise power in (15). This implies that Euclidean distance vector  $u^{QR}$  reflects the instantaneous noise sample power. Let  $\psi^{[i]}$  be a instantaneous noise sample power indicator at  $i$ -th detection layer, and we calculate it as follows:

$$\psi^{[i]} = \frac{|r_{N-i+1,N-i+1}|^2}{u^{QR}}. \tag{16}$$

If  $u_{N-i+1}^{QR}$  decreases owing to the high SNR, then  $\psi^{[i]}$  becomes large, and vice versa. Finally, by multiplying two channel indicators  $\xi^{[i]}$  and  $\psi^{[i]}$ , the total channel condition indicator at  $i$ -th detection layer  $\lambda^{[i]}$  is calculated as follows:

$$\lambda^{[i]} = \xi^{[i]} \psi^{[i]} = \frac{1}{N} \frac{|r_{N-i+1,N-i+1}|^2}{u^{QR}} / \sum_{k=1}^N |r_{k,k}|^2. \tag{17}$$

As SNR increases,  $\xi^{[i]}$  increases and  $u_{N-i+1}^{QR}$  decreases, and thus  $\lambda^{[i]}$  increases. According to calculated  $\lambda^{[i]}$ , the number of candidate symbols at each layer is adaptively controlled.

Meanwhile, the proposed algorithm employs four-Mode adaptation according to  $\lambda^{[i]}$ . Figure 4 shows an example of four-Mode adaptation of the proposed algorithm based on  $\lambda^{[i]}$  with 16QAM at  $i$ -th detection layer. In Figure 4,  $\hat{d}^{[i]}$  is the hard decision symbol by QRD and by comparing  $\lambda^{[i]}$  to three predetermined thresholds  $\lambda_{low}$ ,  $\lambda_{mid}$ , and  $\lambda_{high}$ .

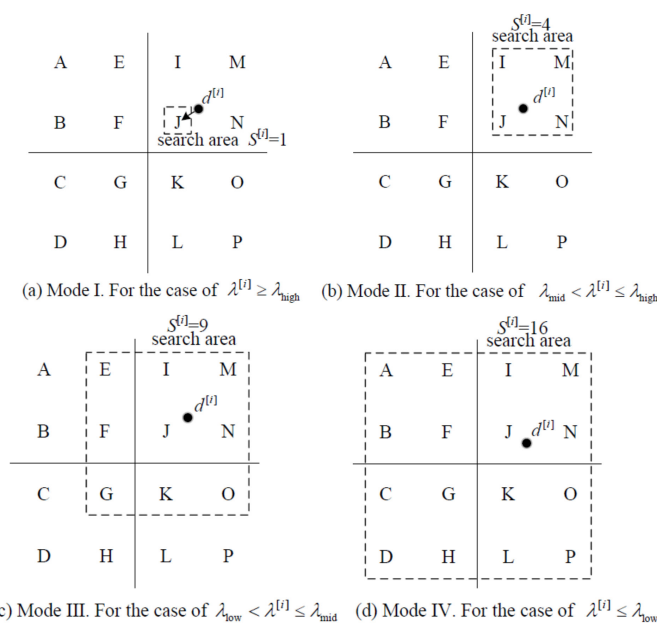


Figure 4. Example of four-Mode adaptation of the proposed scheme.

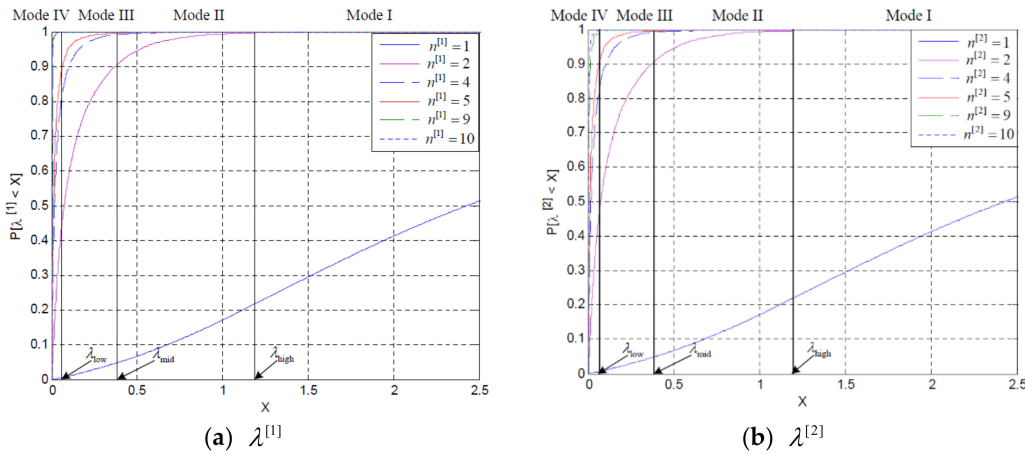
Depending on which range  $\lambda^{[i]}$  belongs to, we determine how many neighboring symbols of  $d^{[i]}$  we will include in the candidate symbol set. The proposed algorithm's adaptation criterion is given as follows:

1. If  $\lambda^{[i]} > \lambda_{\text{high}}$ , we decide that the channel condition is excellent, and thus the estimated symbol is very close to the correct symbol  $\Rightarrow$  set mode I, where  $S^{[i]} = 1$ .
2. If  $\lambda_{\text{mid}} < \lambda^{[i]} < \lambda_{\text{high}}$ , we decide that the channel condition is good, and thus the estimated symbol is near to the correct symbol  $\Rightarrow$  set mode II, where  $S^{[i]} = 4$ .
3. If  $\lambda_{\text{low}} < \lambda^{[i]} < \lambda_{\text{mid}}$ , we decide the channel condition is normal, and thus we have to increase the range of search area  $\Rightarrow$  set mode III, where  $S^{[i]} = 9$ .
4. If  $\lambda^{[i]} < \lambda_{\text{low}}$ , we decide the channel condition is bad, and thus the estimated symbol might be far off from the correct symbol  $\Rightarrow$  set mode IV, where  $S^{[i]} = 16$ .

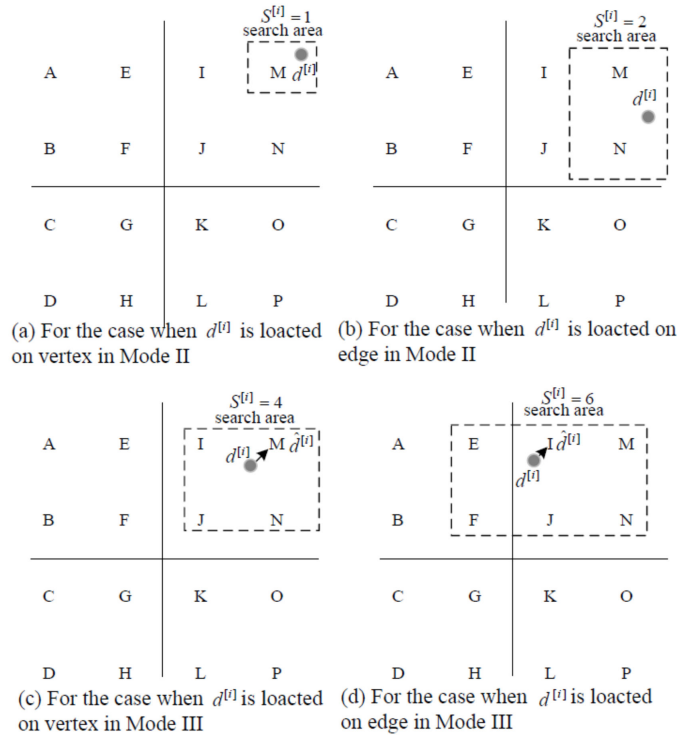
As the threshold values  $\lambda_{\text{low}}$ ,  $\lambda_{\text{mid}}$ , and  $\lambda_{\text{high}}$  determine the computation complexity and detection performance, it is crucial to properly set their values so that the probability of the selected  $S^{[i]}$  neighboring candidate symbols including the correct symbol is high, but the margin should be tight enough to avoid extra computation. Let  $n^{[i]}$  be the path metric order of the correct path at  $i$ -th detection layer. For example, for the case when the correct path's metric is the second minimum at the third detection layer after sorting the metrics for all constellation symbols, we denote the metric order of the correct path as  $n^{[3]} = 2$ . This implies that the path metric order  $n^{[i]}$  can reflect the channel condition. In order to properly set the threshold values,  $\lambda_{\text{low}}$ ,  $\lambda_{\text{mid}}$ , and  $\lambda_{\text{high}}$  on the channel condition, Figure 5a,b illustrate the cumulative distribution function (CDF) of  $\lambda^{[i]}$  at  $i = 1$  and 2 for the cases when  $n^{[i]} = 1, 2, 4, 5, 9,$  and 10, respectively, with  $N = L = 4, 16$  QAM, and  $E_b/N_0 = 20$  dB. We can observe that the distributions of  $\lambda^{[i]}$  are clearly different according to the order of the correct path's metric orders. The probabilities of  $\lambda^{[i]} > 1.2$  at  $i = 1$  and 2 are nearly zero when  $n^{[i]} \neq 1$ . The probabilities of  $\lambda^{[i]} > 0.4$  at  $i = 1$  and 2 are nearly zero when  $n^{[i]} > 4$ . This feature enables us to efficiently restrict the size of search area. If  $\lambda^{[i]} > 1.2$ , it is highly probable that  $n^{[i]} = 1$ , and thus we can safely set mode I, that is,  $S^{[i]} = 1$ . So, we take  $\lambda_{\text{high}} = 1.2$ . If  $\lambda^{[i]} > 0.4$ , the correct path's metric is hardly larger than the fourth minimum, and thus we can safely set mode II, that is,  $S^{[i]} = 4$ . So, we set  $\lambda_{\text{mid}} = 0.4$ . In a similar way, we set the threshold value between mode III and IV,  $\lambda_{\text{low}} = 0.1$  because the correct path's metric is hardly larger than the ninth minimum for  $\lambda^{[i]} > 0.1$ . While it is clear that  $\lambda^{[i]}$  is distributed in the small valued region for the case of not good channel condition, that is,  $n^{[i]} \gg 1$ , the channel indicator,  $\lambda^{[i]}$ , for the case of good channel condition, that is,  $n^{[i]} \simeq 1$ , is rather widely distributed, including a small valued region. So, their distributions are not as clearly disjointed as desired. This implies that we cannot help a tradeoff between complexity and performance in determining the thresholds,  $\lambda_{\text{low}}$ ,  $\lambda_{\text{mid}}$ , and  $\lambda_{\text{high}}$ . As these thresholds get smaller, we can have more chance to have a small  $S^{[i]}$ , and thus we can reduce the complexity. At the same time, the possibility of bad channel condition becomes non-negligible, and thus we may lose the correct path if we take just a few search regions. The effort to minimize the computational complexity is meaningful only when the required symbol error rate (SER) performance is guaranteed. So, in our criterion, we first try to meet the SER performance, and then take the threshold as small as possible within the range where the SER performance is satisfied. By this criterion, predetermined values are set to  $[\lambda_{\text{low}}, \lambda_{\text{mid}}, \lambda_{\text{high}}] = [0.1, 0.4, 1.2]$ . Thus, we adaptively set  $S^{[i]}$  at each detection layer and effectively decrease the metric computation complexity, while achieving almost the same performance as the conventional QRD-M algorithm with large  $M$ .

Figure 6 illustrates examples of the special cases of the proposed algorithm at Mode II and III when  $d^{[i]}$  is located at the edge in the constellation. From this figure, we can expect the proposed algorithm can additively reduce the computation complexity. In Figure 6a,b, the number of neighboring points of  $d^{[i]}$  is just 1 or 2, instead of 4 in Mode II. Similarly, in Figure 6c,d, the number of neighboring points of  $d^{[i]}$  is just 4 or 6, instead of 9 in Mode III.





**Figure 5.** The cumulative distribution function (CDF) of (a)  $\lambda^{[1]}$  and (b)  $\lambda^{[2]}$  for the cases when  $n^{[i]} = 1, 2, 4, 5, 9, 10$ , respectively, at the first detection layer (with 16 QAM and  $E_S/N_0 = 20$  dB,  $N = L = 4$ ).



**Figure 6.** Examples of the special cases of the proposed limited search area.

Figure 7 illustrates an example of the proposed algorithm’s search tree hierarchy for the case when  $S^{[1]} = 9, S^{[2]} = 4$ , and  $S^{[3]} = 16$  with  $N = L = 4$ , and 16 QAM. At the first detection layer, the redundant complexity is reduced by employing the algorithm [18], and thus  $S^{[1]}$  is set to 9. Then, at the second detection layer, based on (19),  $S^{[2]}$  is set to 4, and thus only four candidate symbols are considered. At the third detection layer, owing to the bad channel state,  $S^{[3]}$  is set to 16. Hence, all candidate symbols are considered at this layer. Finally, at the fourth detection layer, the nearest candidate symbol is chosen based on measurement reflecting good channel condition. The simulation results in the following section show that the average complexity of the proposed algorithm is much lower than that of conventional adaptive search area QRD-M conditioned on the same error performance.

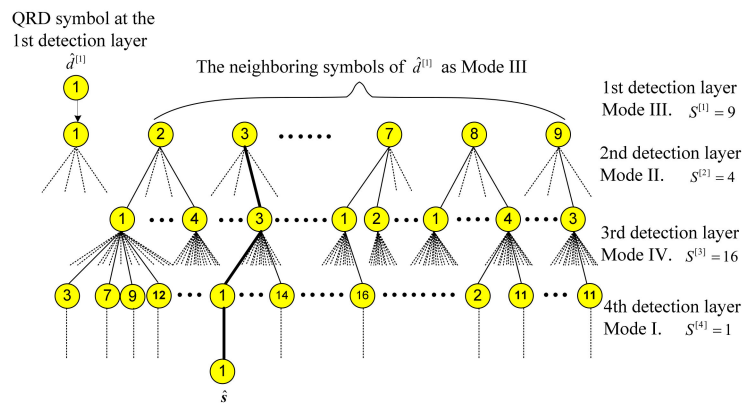


Figure 7. Example of the proposed QRD-M algorithm with  $N = L = 4$  and 16 QAM.

### 6. Simulation Results

This section shows the simulation results to check the performance gain of the proposed QRD-M algorithm. We consider the cases of  $N = L = 3$  and  $N = L = 4$  with 16 QAM and the predetermined values are set to  $[\lambda_{low}, \lambda_{mid}, \lambda_{high}] = [0.1, 0.4, 1.2]$ . For performance comparison, we consider the conventional fixed QRD-M algorithm with  $M = 4$  and 16, and the conventional adaptive search area QRD-M algorithm with  $M = 16$  and MLD. For comparison with the conventional fixed QRD-M algorithm, we select the reduced QRD-M algorithm [18] instead of the conventional fixed QRD-M algorithm because the overall computation complexity is reduced with identical performance. In the sequel, we simply call the full constellation search area QRD-M algorithm ‘reduced QRD-M’. Commonly, in all of the algorithms we consider for comparison, we rearranged the detection order by the norms of the each row in the pseudo inverse of  $\mathbf{H}$  in order to minimize the error propagation effect as done in the ordered detection in successive interference cancellation [23]. As the detection process spends its computation time mainly on metric computations, we take the number of metric computations as the complexity measure. At the last detection layer, we do not contain the metric computation complexity according to [18] and [21].

The SER performances with  $N = L = 3$  and  $N = L = 4$  are shown in Figures 8 and 9, respectively. The proposed algorithm achieves near MLD performance and almost the same performance as the reduced QRD-M algorithm [18] and the conventional adaptive search area QRD-M algorithm based on noise power. However, the conventional fixed QRD-M algorithm with  $M = 4$  significantly deviates from MLD performance owing to the lack of candidate symbols.

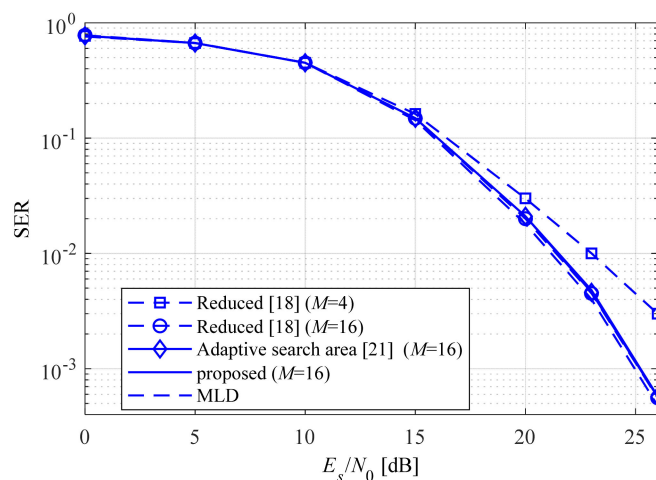


Figure 8. Symbol error rate (SER) performance comparisons for  $N = L = 3$  with 16 QAM. MLD, maximum likelihood detection.

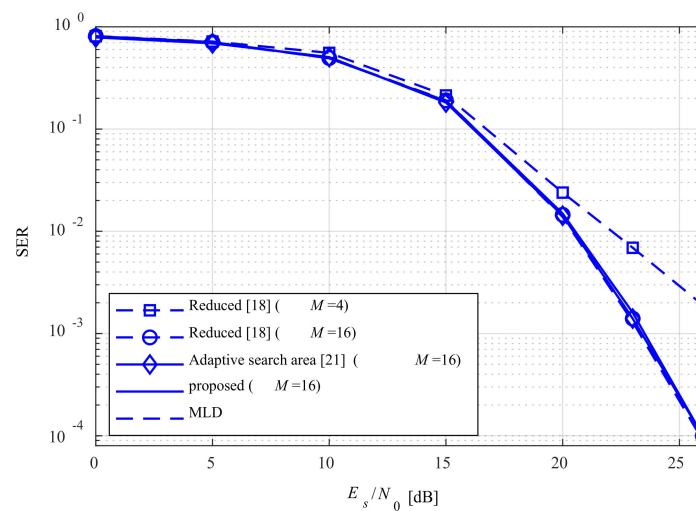


Figure 9. SER performance comparisons for  $N = L = 4$  with 16 QAM.

Figure 10 shows the relative frequencies of the conventional adaptive search area QRD-M algorithm and proposed algorithm with 16 QAM for  $N = L = 4$  at 15 dB and 26 dB, respectively. In Figure 10a, the frequencies of  $S^{[i]} = 16$  are larger than 40% at the first and second detection layer and the frequencies of  $S^{[i]} = 1$  are near to zero at all layers. In Figure 10b, in the case of the proposed algorithm, the frequencies of  $S^{[i]} = 16$  are less than 10% at the second and third detection layer, and the frequencies of  $S^{[i]} = 1$  are larger than 30% at the first and the third detection layer. These results show that the indicator of the proposed algorithm reflects the instantaneous channel condition compared with [21] in a low SNR environment. In Figure 10c, the frequencies of  $S^{[i]} = 1$  of the conventional search area QRD-M algorithm are larger than 70% at all layers, and the frequencies of  $S^{[i]} = 16$  are very low at all layers. From these results, the computation complexity of the conventional adaptive search area QRD-M algorithm significantly decreases compared with the conventional fixed QRD-M algorithm, which achieves the same performance. In Figure 10d, the frequencies of  $S^{[i]} = 1$  in the proposed algorithm are larger than 95% at the second and third detection layer. On the other hand, the frequencies of  $S^{[i]} = 4, 9, \text{ and } 16$  are nearly zero. From these results, we can expect that the proposed algorithm can significantly reduce the computation complexity compared with the conventional adaptive search area QRD-M algorithm as well as the conventional fixed QRD-M algorithm. This is because the frequencies of  $S^{[i]} = 1$  and 16 are the most dominant factors to determine the computational complexity of the systems. These results show that the measurement of the proposed algorithm reflects the instantaneous channel condition compared with [21] even in high SNR conditions.

Figures 11 and 12 show the metric computations' complexity. We can observe that, as SNR increases, the computation complexities of the conventional adaptive search area QRD-M algorithm and the proposed algorithm are significantly reduced compared with the reduced QRD-M ( $M = 4$  and 16). In Figure 11, as expected before, the proposed algorithm achieves more than about 93%, 96.7%, 98.2%, and 99% of the reduction of the metric computation compared with the reduced QRD-M algorithm ( $M = 16$ ) at 15 dB, 20 dB, 23 dB, and 26 dB, respectively, with  $N = L = 3$ . Even compared with the conventional adaptive search area QRD-M algorithm, the proposed algorithm achieves more than about 85%, 72%, 63%, and 46% of the reduction of the metric computation.

Similarly, in Figure 12, the metric computation complexity of the proposed algorithm is significantly decreased compared with the conventional QRD-M algorithms in SNR regions larger than 12 dB with  $N = L = 4$ . The proposed algorithm requires 13.87%, 4.99%, 2.41%, and 1.33% metric computations over the reduced QRD-M ( $M = 16$ ), which achieve the same performance at 15 dB, 20 dB, 23 dB, and 26 dB, respectively. In high SNR ( $E_s/N_0 = 23$  dB, 26 dB), the proposed algorithm achieves more than about 90% and 94.5% of the reduction of the metric computation, even compared with the reduced QRD-M with  $M = 4$ . In the same SER performance condition, the proposed algorithm achieves more

than about 76%, 67%, 52%, and 26% of the reduction of the metric computations compared with the conventional adaptive search area QRD-M algorithm at 15 dB, 20 dB, 23 dB, and 26 dB, respectively. This is because the channel indicator that is used in the proposed algorithm reflects instantaneous channel information about the instantaneous noise power as well as the instantaneous channel fading. On the other hand, noise power that is used as the adaptation indicator in the conventional adaptive search area QRD-M algorithm does not contain the instantaneous channel information.

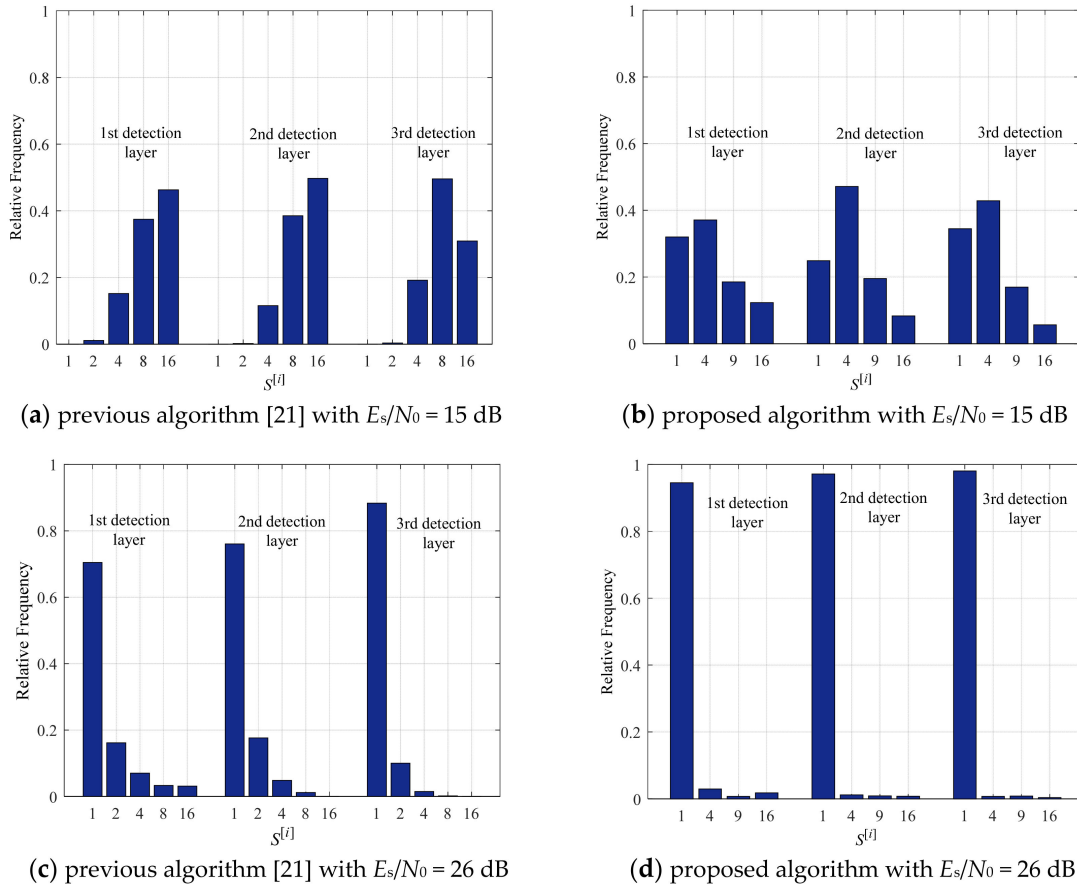


Figure 10. Relative frequencies of the conventional adaptive search area QRD-M [21] and the proposed algorithm for  $N = L = 4$  with 16 QAM at  $i = 1-3$  with 15 dB and 26 dB.

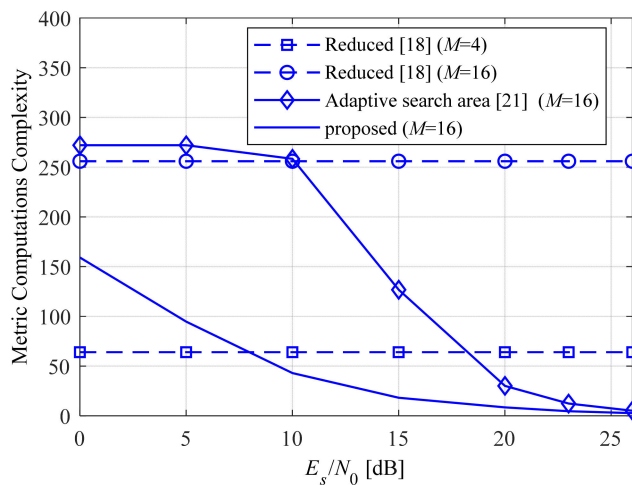


Figure 11. Average metric computation complexity comparisons,  $N = L = 3$  with 16 QAM.

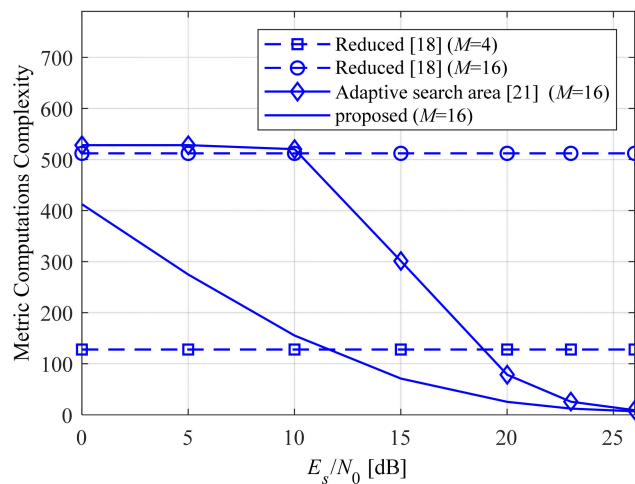


Figure 12. Average metric computation complexity comparisons,  $N = L = 4$  with 16 QAM.

### 7. Discussions

This section addresses the comparison of the QRD-M MIMO detection algorithms. Table 1 shows the summary of the QRD-M algorithms. The fixed QRD-M algorithm [16] is the classical QRD-M algorithm. In [18], they reduced redundant complexity at the first and last layers, but this algorithm did not control survivor paths and search area according to channel conditions. Hence, the effect of the complexity reduction of this algorithm is slight. In [19], this algorithm controlled the number of survivor paths according to measured noise power. In [20], this algorithm adaptively changed the number of survivor paths based on the path metric at each layer. However, [19] and [20] changed not search area, but the survivor paths, and thus the effect of the complexity reduction was not high compared with the schemes that controlled search area. In [21] and this paper, the search area was changed based on noise power and channel conditions. Hence, their effect of complexity reduction was very high.

Table 1. Summary of the QRD-M algorithms.

Article	Mode	Subject to Control	Measurement	Effect of Complexity Reduction
[16]	Fixed	None	None	None
[18]	Fixed	None	None	Slight
[19]	Adaptive	Survivor paths	Noise power	Middle
[20]	Adaptive	Survivor paths	Ratio of paths	Middle
[21]	Adaptive	Search area	Noise power	high
Proposed	Adaptive	Search area	Ratio of diagonal matrix and partial Euclidean distance	high

### 8. Conclusions

We proposed a new low complexity QRD-M algorithm based on adaptive search area for MIMO systems. The proposed algorithm significantly decreases the computational complexity compared with the conventional adaptive search area QRD-M algorithm based on average noise power as well as the conventional fixed QRD-M algorithm, while achieving near MLD performance. This is because the proposed algorithm adaptively changes the range of the search area using a channel indicator, which contains the instantaneous noise power as well as the instantaneous channel fading. We can expect further complexity reduction if the proposed algorithm is jointly performed with the adaptation of the number of survivor paths based on instantaneous channel information, which is also on-going by the authors.

**Author Contributions:** All authors conceived and designed the system and experiments together; B.-s.K., S.-D.K., D.N., and K.C. performed the simulations and analyzed the results. All authors have read and agreed to the published version of the manuscript.

**Funding:** This work was supported by the DGIST R&D Program of the Ministry of Science, ICT, and Future Planning, Korea (20-IT-02), the Brain Korea 21 Plus Program(No. 22A20130012814) funded by the National Research Foundation of Korea (NRF) and the 2020 Yeungnam University Research Grant.

**Conflicts of Interest:** The authors declare no conflict of interest.

## References

1. Jankiraman, M. *Space-Time Codes and MIMO Systems*; Artech House: London, UK, 2004.
2. Ali, M.S.; Ehosai, N.; Kim, D. Non-Orthogonal Multiple Access (NOMA) for Downlink Multiuser MIMO Systems: User Clustering, Beamforming, and Power Allocation. *IEEE Access* **2017**, *5*, 565–577. [[CrossRef](#)]
3. Spencer, Q.; Peel, C.B.; Swindlehurst, A.L.; Haardt, M. An Introduction to the Multi-User MIMO Downlink. *IEEE Commun. Mag.* **2004**, *42*, 60–67. [[CrossRef](#)]
4. Wong, K.; Cheng, R.; Letaeif, K.B.; Murch, R.D. Adaptive antennas at the mobile and base stations in an OFDM/TDMA system. *IEEE Trans. Commun.* **2001**, *49*, 195–206. [[CrossRef](#)]
5. Zhai, K.; Zheng, M.A.; Lei, X. Accurate Performance Analysis of Coded Large-Scale Multiuser MIMO Systems with MMSE Receivers. *Sensors* **2019**, *19*, 2884. [[CrossRef](#)] [[PubMed](#)]
6. Naeem, M.; Bashir, S.; Ullah, Z.; Syed, A.A. A Near Optimal Scheduling Algorithm for Efficient Radio Resource Management in Multi-user MIMO Systems. *Wirel. Pers. Commun.* **2019**, *106*, 1411–1427. [[CrossRef](#)]
7. Tseng, S.M.; Chen, Y.F. Average PSNR optimized cross layer user grouping and resource allocation for uplink MU-MIMO OFDMA video communications. *IEEE Access* **2018**, *6*, 50559–50571. [[CrossRef](#)]
8. Vanidevi, M.; Selvaganesan, N. Fast iterative WSVT algorithm in WNN minimization problem for multiuser massive MIMO channel estimation. *Int. J. Commun. Syst.* **2018**, *31*, E3378. [[CrossRef](#)]
9. Li, J.-F.; Chu, Q.-X.; Li, Z.-H.; Xia, X.-X. Compact Dual Band-Notched UWB MIMO Antenna with High Isolation. *IEEE Trans. Antennas Propag.* **2013**, *61*, 4759–4766. [[CrossRef](#)]
10. Yang, J.O.; Yang, F.; Wang, Z.M. Reducing Mutual Coupling of Closely Spaced Microstrip MIMO Antennas for WLAN Application. *IEEE Trans. Antennas Propag.* **2011**, *10*, 310–313. [[CrossRef](#)]
11. Zhu, F.; Xu, J.; Xu, Q. Reduction of mutual coupling between closely packed antenna elements using defected ground structure. *IET Electron. Lett.* **2009**, *45*, 601–602. [[CrossRef](#)]
12. Alibakhshikenari, M.; Virdee, B.S.; See, C.H.; Abd-Alhameed, R.; Ali, A.H.; Falcone, F.; Limiti, E. Study on Isolation Improvement Between Closely Packed Patch Antenna Arrays Based on Fractal Metamaterial Electromagnetic Bandgap Structures. *IET Microw. Antennas Propag.* **2018**, *12*, 2241–2247. [[CrossRef](#)]
13. Yasser, F.; Abdeldjalil, A.; Karine, A.; Dominique, P.; Ramesh, P. New iterative detector of MIMO transmission using sparse decomposition. *IEEE Trans. Veh. Technol.* **2015**, *64*, 3458–3464.
14. Jalden, J.; Ottersten, B. An Exponential Lower Bound on the Expected Complexity of Sphere Decoding. In Proceedings of the IEEE ICASSP 2004, Montreal, QC, Canada, 17–21 May 2004.
15. Damen, M.O.; el Gamal, H.; Caire, G. On Maximum-Likelihood Detection and the Search for the Closest Lattice Point. *IEEE Trans. Inform. Theory* **2003**, *49*, 2389–2402. [[CrossRef](#)]
16. Chin, W.H. QRD based tree search data detection for MIMO communication systems. In Proceedings of the VTC 2005-Spring, Stockholm, Sweden, 30 May–1 June 2005.
17. Peing, W.; Ma, S.; Ng, T.S.; Wang, J.Z. Adaptive QRD-M Detection with variable number of surviving paths for MIMO systems. In Proceedings of the ISCIT 2007, Sydney, Australia, 17–19 October 2007.
18. Im, T.; Kim, J.; Cho, Y. A low complexity QRM-MLD for MIMO systems. In Proceedings of the IEEE VTC 2007-Spring, Dublin, Ireland, 22–25 April 2007.
19. Kawai, H.; Higuchi, K.; Maeda, N.; Sawahashi, M. Adaptive control of surviving symbol replica candidates in QRM-MLD for OFDM MIMO multiplexing. *IEEE J. Select. Areas Commun.* **2006**, *24*, 1130–1140. [[CrossRef](#)]
20. Kim, B.; Choi, K. Adaptive tree search algorithm based on path metric ratio for MIMO systems. *IEICE Trans. Commun* **2011**, *E94-B*, 997–1005. [[CrossRef](#)]
21. Lai, K.; Lin, L. Low-Complexity Adaptive Tree Search Algorithm for MIMO Detection. *IEEE Wirel. Commun.* **2009**, *8*, 3716–3726. [[CrossRef](#)]



22. Kim, B.; Choi, K. Low complexity QRD-M MIMO detection algorithm based on adaptive search area. *J. KICS* **2008**, *33*, 614–623.
23. Wolniansky, P.W.; Foschini, G.J.; Golden, G.D.; Valenzuela, R.A. V-BLAST: An architecture for realizing very high data rates over the rich-scattering wireless channel. In Proceedings of the URSI ISSSE, Pisa, Italy, 2 October 1998.



© 2020 by the authors. Licensee MDPI, Basel, Switzerland. This article is an open access article distributed under the terms and conditions of the Creative Commons Attribution (CC BY) license (<http://creativecommons.org/licenses/by/4.0/>).